

**Keywords:** crane; dynamics; modeling; simulation; vibration; rope

**Tomasz HANISZEWSKI**

Silesian University of Technology, Faculty of Transport  
Krasinskiego 8, 40-019 Katowice, Poland  
*Corresponding author.* E-mail: [tomasz.haniszewski@polsl.pl](mailto:tomasz.haniszewski@polsl.pl)

## **PRELIMINARY MODELLING STUDIES OF AN EXPERIMENTAL TEST STAND OF A CRANE, FOR INVESTIGATION OF ITS DYNAMIC PHENOMENA OF LIFTING AND DRIVING MECHANISM**

**Summary.** In the article, the problem of designing and preliminary tests on experimental test bench was taken into account. Proposed test stand allows us to carry out a series of studies concerning the dynamic phenomena accompanying the lifting of the load. Presented test bench allows, among other things, measurements of data such as the acceleration of selected points of the girder and also of cargo, displacement of cargo and centre of the girder, along with measurement of stress in selected locations and the coefficient of dynamic surplus. The electronic part of the test bench was made using the PHIDGET and the Arduino platform. Owing to the full miniaturization and implementation of control and measurement systems from the application level, test stand allows testing new mechanisms for implementing control algorithms and studying the influence of control parameters on the values of dynamic coefficients characterizing the selected dynamic mechanisms. Such an approach provides the possibility, among other things, of full control of the systems using a computer, and thus an immediate analysis of the data, which is extremely important in process of verification in the phenomenological model creation of the analyzed crane mechanisms. The proposed approach enables the development of existing ones and testing new design solutions in scale (experimental) and pure software solutions (analytical).

### **1. INTRODUCTION**

One of the problems in the process of constructing physical models of machines mechanisms is the verification of analytically obtained data with experimental results. By concentrating on cranes, a model of an experimental test bench with a span of 4 m was proposed. Because of the wide span of the girder, which is the beam, the load lifting process is accompanied by a certain amount of dynamic surplus [8, 13] determined by the normative [21]. This value is related to the vertical movement of the load. The values of additional deflections or dynamic stresses caused by these deflections are particularly disclosed when the load, i.e, cargo, is in the middle of the span of the supporting structure [3, 12, 15, 18].

Determining the value of dynamic forces can create some difficulties [9]. It can be done experimentally or by analytical methods, which can be verified by an experiment. For research purposes, the following section presents the design and model of an experimental test stand. The aim is to allow for a number of studies related to the dynamics of the cranes. Due to the fact that most values of dynamic loads are levelled by the appropriate motor control algorithm, both the lifting mechanisms and the bridge and trolley mechanisms, the test stand has been designed to remotely set and control the signals for the lifting and driving mechanisms. These algorithms or any other technical solutions enabling reduction of harmful dynamic loads must be supported by either the number of

studies referenced or the studies on the real object, which led to the proposed test stand. It is important that these studies must be conducted in the most extreme cases, random cases or for standard loads repeatedly performed during the operation of the machine, which in most cases is not possible on a real object due to the time spent on his work.

## 2. DESCRIPTION OF TEST STAND

The purpose of this article is to present the construction and initial testing of a mechatronic model of a bridge crane with particular emphasis on the lifting mechanism and its control. As it is known, the cranes are characterised by work with intermittent motion, the loads are therefore caused by the acceleration or deceleration of the work movement and are considered to be a regular load. Hence, lifting the load from the ground or releasing it causes vibration of the hoist structure [3, 5, 13, 14, 19, 20]. Table 1 shows the general characteristics of the tested overhead traveling crane, which was prepared on the basis of the technical documentation.

Table 1

Characteristics of experimental crane

description	Symbol	dimension	value
lifting capacity	Q	[kg]	80
span	L	[m]	4
lifting height	$H_{p \max}$	[m]	2
operating speed	lifting	$v_h$	[m/s]
	winch driving	$v_{jw}$	[m/s]
supply voltage	U	[V]	220

Mechatronic models of cranes are a rare solution in relation to the objectives of research, especially regarding the dynamics of the lifting mechanism. Its main purpose is to study the dynamic behavior of the lifting mechanism while lifting the load, i.e., lifting from the ground, lifting of frozen cargo, jerking due to lack of control of the winding speed of the rope on the drum, dump of the mass or part of it, breaking and many other cases, which in varying degrees affect the so-called coefficient of dynamic surplus ratio.

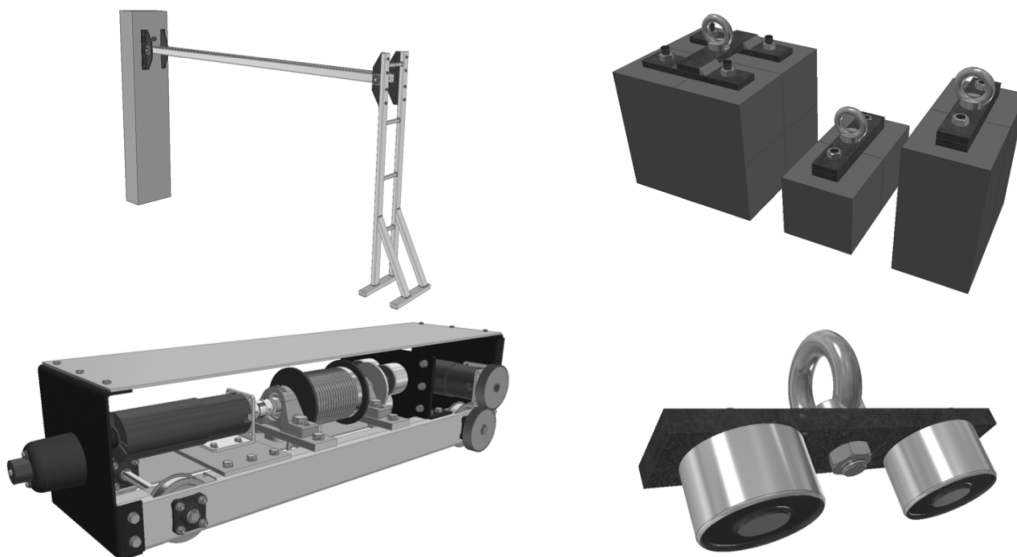


Fig. 1. 3D model of, a) an experimental test stand, b) set of test loads, c) trolley with lifting and driving mechanism, and d) electromagnetic grip

The test stand was pre-designed in 3D CAD software, which is presented in Fig. 1. Then the model was made of standard steel sections and sheets. The lifting system consists of a DC motor with an optical encoder on the second shaft, and the motor is equipped with an integrated planetary gear with a ratio 76:1.



Fig. 2. Experimental test stand

The motor is connected by a flexible coupling to the cable drum and equipped with an electromagnetic brake. On the trolley, the limit switches, the driving mechanism of the travel mechanism and the entire control system together with the inverters on the top plate of the trolley are also included. Engine control system for both lifting and trolley driving has a possibility to control the angular velocity of the motor shaft and in conjunction with software PID controller allows to determine the exact position of the load and thus enables its positioning [16]. In the construction of the trolley (Fig. 3), an accelerometer and gyroscope system for measuring angular velocity and acceleration in three independent axes were also assembled; additional accelerometers and gyroscopes are used at the ends of the girder and the wireless system on the test load to measure acceleration and angles in motion and impact situation. [2, 4]. Subsequently, strain gauges were used to determine the force in the rope and load pressure gauges on the ground for the verification of load raising condition (Fig. 7).

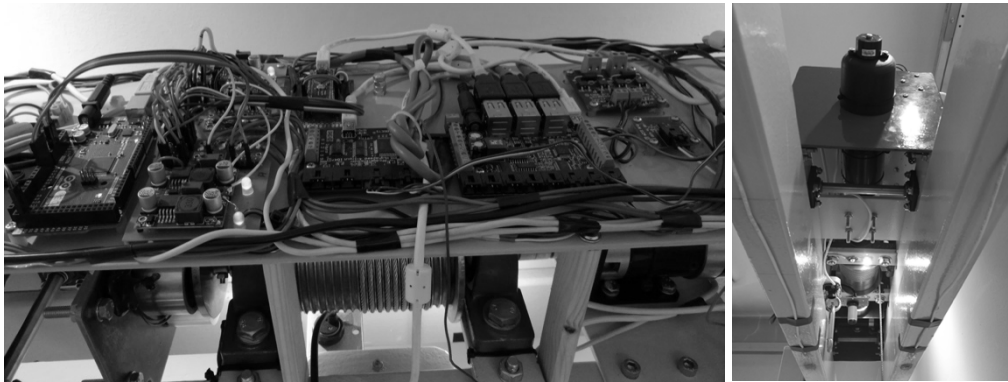


Fig. 3. Trolley – control and power supply systems, a) top view, b) view from the bottom

During the construction of the girder, a series of permanently installed strain gauges were used to provide tension values at selected locations. The entire test stand is controlled from a PC using USB ports; the power supply was based on three industrial power supplies of 12 and 24 V DC. Additionally, two gel batteries were used as protection system for receiving power generated during lowering the load. They were also included in the brake control system of lifting mechanism.

### 3. NUMERICAL MODEL OF LIFTING MECHANISM

The phenomenological model of the experimental crane is shown in Fig. 4. This model contains in its structure, the girder, the drum, the rope and the ground on which the load rests.

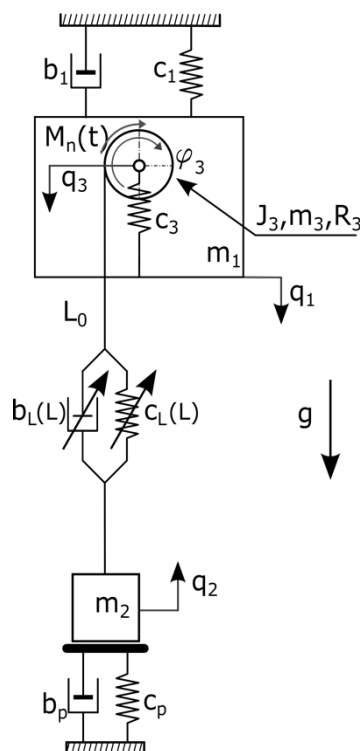


Fig. 4. Simplified phenomenological model of examined overhead travelling crane

On the basis of the concept of generalised coordinates, and phenomenological model shown in Fig. 4, the equations of motion can be written as second type Lagrange equations [1, 6, 17]:

$$\frac{d}{dt} \left( \frac{\partial E_k}{\partial \dot{q}_j} \right) - \frac{\partial E_k}{\partial q_j} + \frac{\partial E_p}{\partial q_j} + \frac{\partial E_R}{\partial \dot{q}_j} = F_j, \quad j = 1, 2, \dots, n \quad (1)$$

where  $t$  – time,  $q_j$  – generalized displacement,  $\dot{q}_j$  – generalized velocity,  $n$  – number of degrees of freedom,  $F_j$  – generalized force,  $E_k$  – kinetic energy,  $E_p$  – potential energy, and  $E_R$  – Rayleigh dissipation function.

This approach allows obtaining the differential equations of motion in the following form:

$$\begin{aligned} & \begin{vmatrix} m_1 & 0 & 0 & 0 \\ 0 & m_2 & 0 & 0 \\ 0 & 0 & m_3 & 0 \\ 0 & 0 & 0 & J_3 \end{vmatrix} \begin{vmatrix} \ddot{q}_1 \\ \ddot{q}_2 \\ \ddot{q}_3 \\ \ddot{\varphi}_3 \end{vmatrix} + \begin{vmatrix} b_1 & 0 & 0 & 0 \\ 0 & (b_p + b_L(L)) & b_L(L) & -b_L(L)R_3i_w^{-1} \\ 0 & b_L(L) & b_L(L) & -b_L(L)R_3i_w^{-1} \\ 0 & -b_L(L)R_3i_w^{-1} & -b_L(L)R_3i_w^{-1} & b_L(L)R_3^2i_w^{-2} \end{vmatrix} \begin{vmatrix} \dot{q}_1 \\ \dot{q}_2 \\ \dot{q}_3 \\ \dot{\varphi}_3 \end{vmatrix} + \\ & + \begin{vmatrix} (c_1 + c_3) & 0 & -c_3 & 0 \\ 0 & (c_p + c_L(L)) & c_L(L) & -c_L(L)R_3i_w^{-1} \\ -c_3 & c_L(L) & (c_3 + c_L(L)) & -c_L(L)R_3i_w^{-1} \\ 0 & -c_L(L)R_3i_w^{-1} & -c_L(L)R_3i_w^{-1} & c_L(L)R_3^2i_w^{-2} \end{vmatrix} \begin{vmatrix} q_1 \\ q_2 \\ q_3 \\ \varphi_3 \end{vmatrix} = \begin{vmatrix} 0 \\ -m_2g \\ 0 \\ M_n(t) \end{vmatrix} \end{aligned} \quad (2)$$

where  $c_3$  – stiffness coefficient of the cable drum axle,  $c_p$  – stiffness coefficient of ground,  $b_p$  – damping coefficient of ground,  $c_1$  – stiffness coefficient of the girder,  $b_1$  – damping coefficient of the girder,  $c_L(L)$  – stiffness coefficient of wire rope,  $b_L(L)$  – damping coefficient of wire rope,  $R_3$  – radius of the cable drum,  $i_w$  – gear ratio of pulley blocks, and  $q_1, q_2, q_3, \varphi_3$  – generalized displacements.

Rope stiffness coefficient was defined by the relation (3), and its value depends on the length of the rope (Fig. 5):

$$c_L(L) = \frac{n_{lin} \cdot A_l E_l}{L(t)} = \frac{n_{lin} \cdot A_l E_l}{(L_0 - R_3 \varphi_3(t))} \quad \text{where: } E_l = (0,4 \div 0,65) E_s \quad (3)$$

where  $n_{lin}$  – number of bands of wire rope,  $L_0$  – initial length of the rope,  $E_l$  – modulus of elasticity,  $A_l$  – cross sectional area of wire rope,  $E_s$  – Young modulus for steel.

Variable damping coefficients of wire rope strand are taken from the publications of Čech M. et al. and Kim et al. [7, 12]:

$$b_L(L) = 2\zeta \sqrt{c_L(L) (m_2 + n_{lin} \rho_l A_l (L_0 - R_3 \varphi_3(t)))} \quad (4)$$

where  $\zeta$  – dimensionless coefficient,  $\rho_l$  – density of steel.

The reaction of the ground  $N$  is dependent on displacement and velocity. Value of  $N$  is a sum of  $N_{cp}$  and  $N_{bp}$ . At rest, the elastic force and the damping force of the ground affect the cargo. At the time of lifting load, the force will be switched off from the system. The value of this reaction is described below:

$$N_{cp} = \begin{cases} 0 & q_2 \geq 0 \\ -c_p q_2 & q_2 < 0 \end{cases} \quad N_{bp} = \begin{cases} 0 & \dot{q}_2 \geq 0 \\ -b_p \dot{q}_2 & \dot{q}_2 < 0 \end{cases} \quad (5)$$

where:  $N_{cp}$  – elastic part of ground reaction,  $N_{bp}$  – damping part of ground reaction.

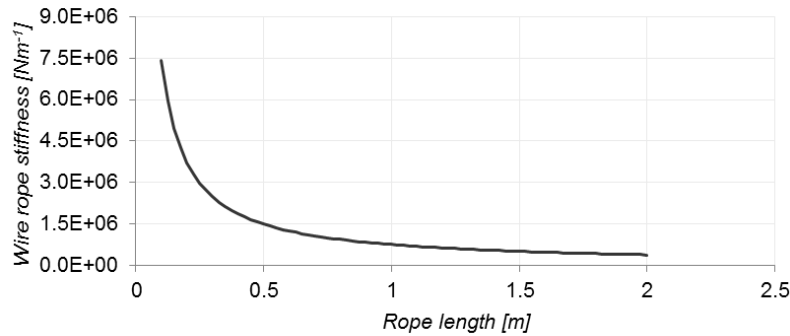


Fig. 5. Diagram of rope stiffness change due to shortening and elongation of the wire rope

In Matlab-Simulink environment, the dynamic model was formulated. Table 2 shows the physical parameters describing the considered vibrating model, which is estimated on the basis of the technical documentation. Then the numerical experiments for the data presented and the assumed initial conditions with the classical model of the elastic-damping model (Kelvin-Voigt) for the wire rope were performed. As the extortion signal was used a constant driving torque corresponding to the fast start of the engine, without the control system, ie. the worst case. In accordance with the applicable standard [21], the hoist drive class HD1 (Fig. 6) [3], for the lifting mechanisms without creep speed, was examined.

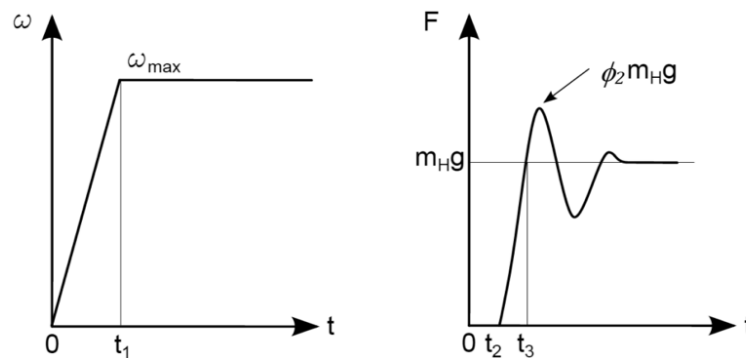


Fig. 6. Hoist drive class HD1 in the function of angular velocity  $\omega$  and the resulting lifting force  $F$ , where:  $t = 0$  – start of drive,  $t_1 - \omega = \omega_{max}$ ,  $t_2$  – start of rope tightening ( $t_2 \rightarrow 0$ ),  $t_3$  – start of load lifting,  $m_H$  – cargo mass

Simulations were carried out using algorithm ode4, with constant step of integration  $1E-05$  s. Simulations were performed for a load value of 22.6 kg. After a series of numerical experiments, many model parameters were obtained, such as girder acceleration in different points.

#### 4. SIMULATION AND TEST STAND TESTS

A number of experiments were performed on presented research bench. For research purposes, a test load of mass 22.6 kg was used, as shown in Fig. 7, 8. The research program consists of determining the acceleration values at the four selected points, including the girders. The sensor layout is shown in Fig. 8.

Table 2

Physical parameters describing the dynamic system

No.	Symbol	Value	Unit	No.	Symbol	Value	Unit
1	$m_1$	44	[kg]	13	$L_0$	2	[m]
2	$m_2$	22,6	[kg]	14	$A_1$	2,826e-5	[m <sup>2</sup> ]
3	$m_3$	1	[kg]	15	$\rho_l$	7850	[kg/m <sup>3</sup> ]
4	$m_{linv}$	2.22	[kg]	16	$E_s$	2,1e011	[Pa]
5	$J_3$	0,0039	[kgm <sup>2</sup> ]	17	$E_l$	1,155e011	[Pa]
6	$c_1$	4e5	[N/m]	18	$g$	9,81	[m/s <sup>2</sup> ]
7	$c_p$	2,0e8	[N/m]	19	$V_p$	0,12	[m/s]
8	$c_3$	1,8e8	[N/m]	20	$n_{lin}$	1	[-]
9	$b_p$	1,0e6	[Ns/m]	21	$\zeta$	0,07	[-]
10	$b_1$	2e3	[Ns/m]	22	$i_w$	1	[-]
11	$R_3$	0,08	[m]				
12	$d_l$	0,003	[m]				

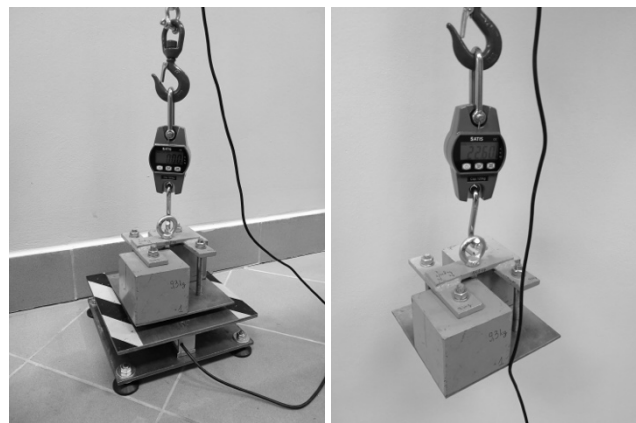


Fig. 7. Test load on a sensor used for verifying the state of lifted load

The test program consisted of raising the load from the ground assuming a loose rope during the initial phase of the lifting process. The second test case was the sudden release of the load using the electromagnetic head between the load and the hook (Fig. 1d).

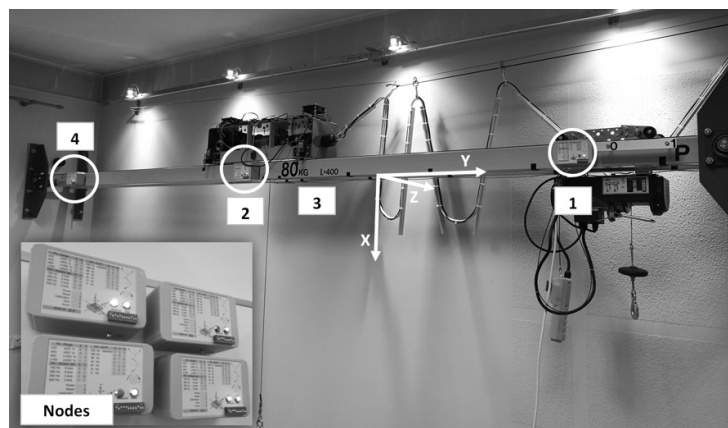


Fig. 8. Measurement nodes setup on a test stand

#### 4.1. Research results from test stand

The measurements were made using an experimental set of wireless accelerometers based on the MPU6050 sensor, with a resolution of 16 bit with sampling rate about 250 Hz for a 3-measurement axis (Fig. 8). In the further part of the study, these sensors will be called measurement nodes [7, 11]. Data were recorded using the Bluetooth interface on a laptop computer. Measurement nodes are set up, as in Fig. 8, on the left and right sides of the front girder and in the middle position of the girder on both the front and rear. The results are detailed in the drawings 9, 10.

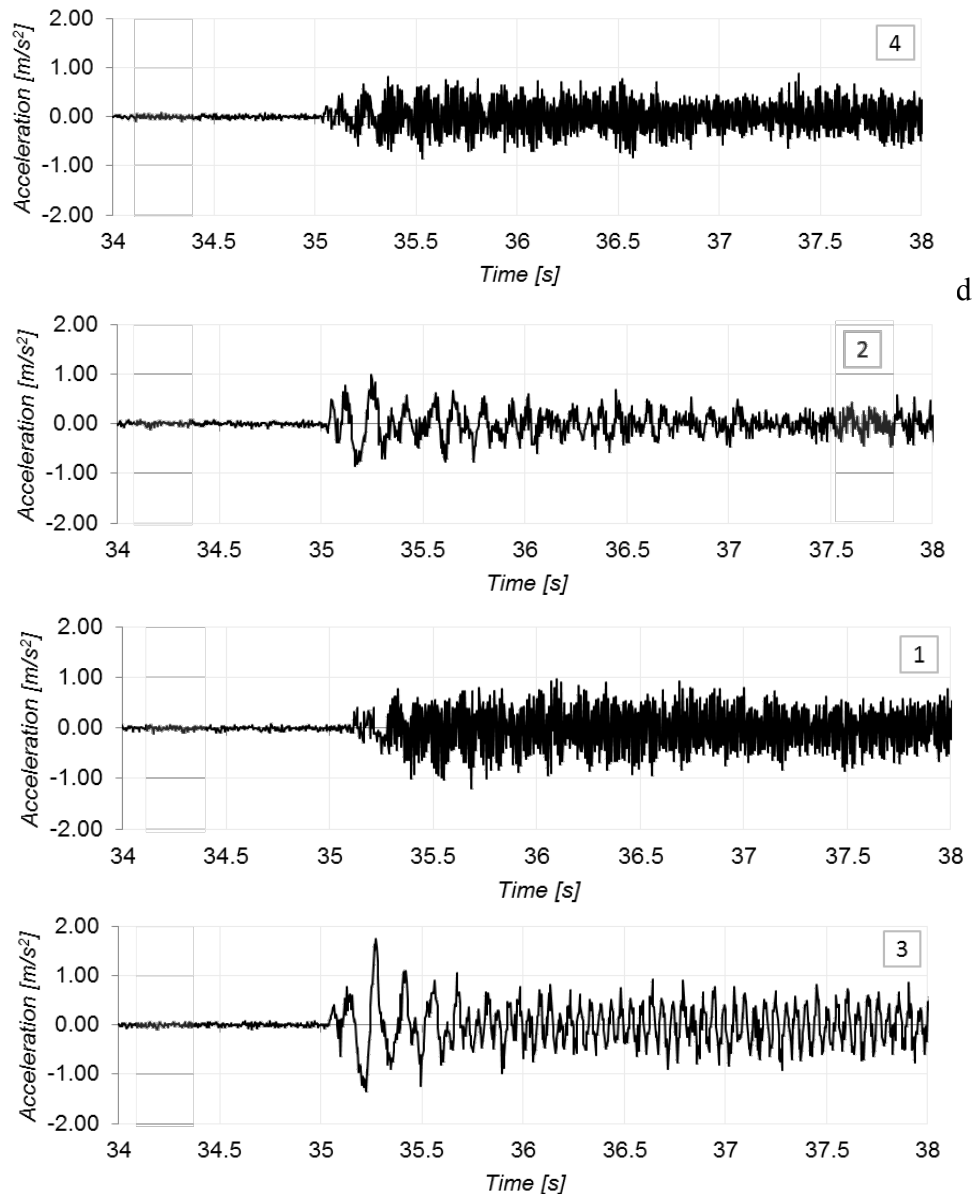


Fig. 9. The acceleration of the girder in axis of lifting at position – lifting the load with loose rope, 1) right end position, 2) centre of the front girder, 3) centre of the rear girder, and 4) left end position

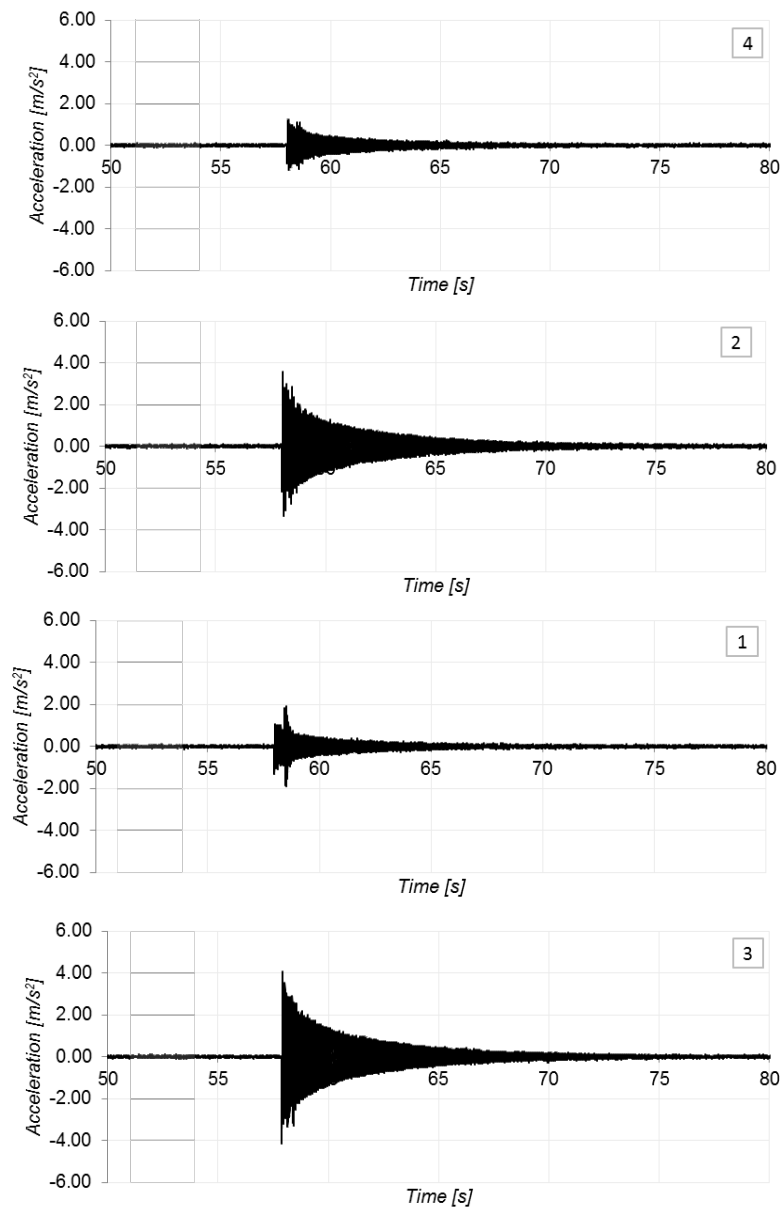


Fig. 10. The acceleration of the girder in axis of lifting at position - sudden release of cargo, 1) right end position, 2) centre of the front girder, 3) centre of the rear girder, 4) left end position

The graphs show a significant increase in acceleration, especially in the case of sudden release of the load, where acceleration values reach  $4 \text{ m/s}^2$  for the centre of the girder and  $2 \text{ m/s}^2$  for the extreme lateral positions. For the case of the load pickup, in spite of the pickup and loose rope, acceleration is small and is located on the boundary between  $1 \text{ m/s}^2$  and  $2 \text{ m/s}^2$ , which is closely connected to the structure of the lifting mechanism, i.e., a small angular velocity of the motor.

#### 4.2. Results of numerical tests

Using the presented phenomenological model, a number of numerical studies have been carried out including load lifting and sudden release of cargo. The results of the simulations are shown in the Fig. 11 and 12, in the form of a displacement of the centre of the girder and its acceleration as a function of time.

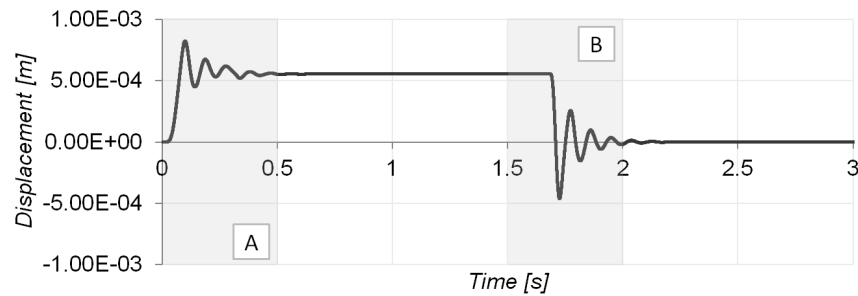


Fig. 11. The displacement of the girder centre in axis of lifting, a) start zone, b) sudden release of cargo

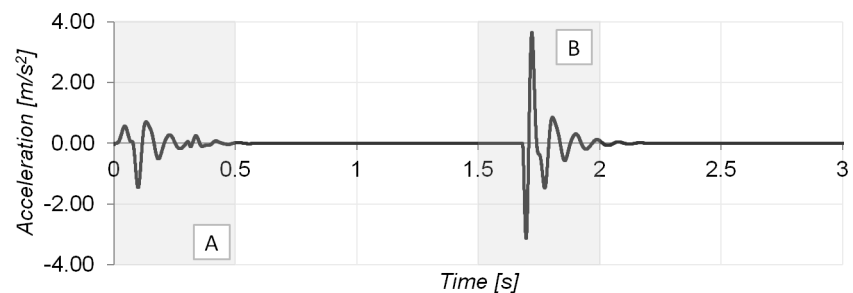


Fig. 12. The acceleration of the girder centre in axis of lifting, a) start zone, b) sudden release of cargo

As can be seen in Fig. 12, acceleration values in the start-up phase reach values 1 – 1.5  $\text{m/s}^2$ , whereas for the sudden release of cargo these values reach 3 to 4  $\text{m/s}^2$ . As shown in Fig. 11 and 12, these values are similar to those obtained by experimenting on a real object (Fig. 9, 10).

## 5. CONCLUSIONS

As presented in the paper, experimental research stand allows carrying out several studies typically associated with the dynamics of hoist mechanisms. As shown, results from the preliminary research and values obtained by numerical experiments are similar, which shows a good fit of the numerical model. The test stand still requires some modifications to fully use its capabilities. These changes mainly involve the software part, e.g., work control and automation of control of executive mechanisms. After modifications in both the software side and the hardware side, e.g. replacement of a lifting mechanism motor, it allows carrying out load lifting simulations with significant values of dynamic surpluses. Assembly of the motor with higher torque and angular speed is not a problem because of the adaptation of the supporting structure itself to higher load values.

The appropriately adapted software will also allow for continuous reading and gathering of other data provided by a number of sensors used on the test bench. Currently accessible data from the object are values of stresses in both beams in the middle of the span, acceleration of the hoisting mechanism, verification of weight and load condition, measurement of dynamic overload factor value during lifting, lifting speed, angular speed of the rope drum, angular velocity of driving and lifting motors, the temperature of the motors and planetary gears and the environment, measurement of the distance from the support to the support, measurement of impact force on bumpers and measurement of the output current. Mounted control unit allows monitoring and control mechanism of driving, lifting, release of the cargo, the camera view of the lifting mechanism and brake control of the lifting mechanism.

After the preliminary tests, it is stated that the experimental test stand for the study of the dynamics of the operating mechanisms of the overhead cranes fulfils its role, giving great opportunities for verification of tests on the proposed phenomenological models of these mechanisms. Proposed test

stand, being a mechatronic model of the crane, is therefore applicable to assess the effectiveness of elimination of mechanical vibration transmitted to the structure during load lifting for different methods of controlling the angular velocity of the motor.

## References

1. Cannon, R.H. *Dynamics of physical systems*. Warszawa: WNT. 1973. 930 p.
2. Kucharski, T. *System pomiaru drgań mechanicznych*. Warszawa: WNT. 2002. [In Polish: *Mechanical vibration measurement system*].
3. Margielewicz, J. & Haniszewski, T. & Gąska, D. & Pypno, C. *Badania modelowe mechanizmów podnoszenia suwnic*. Katowice: Polish Academy of Science. 2013. 204 p. [In Polish: *Model studies of cranes hoisting mechanisms*].
4. Osiecki, J. & Ziemba, S. *Podstawy pomiarów drgań mechanicznych*. Warszawa: PWN. 1968. [In Polish: *Basics of mechanical vibration measurements*].
5. Piątkiewicz, A. & Sobolski, R. *Dźwignice*. Warszawa: WNT. 1978. [In Polish: *Cranes*].
6. Bogdevičius, M. & Vika, A. Investigation of the dynamics of an overhead crane lifting process in a vertical plane. *Transport*. 2005. Vol. 20(5). P. 176-180.
7. Čech, M. & Schlegel, M. & Balda, P. & Reitingner, J. New tools for teaching vibration damping concepts: ContLab.eu. *IFAC Proceedings Volumes*. 2014. Vol. 47. No. 3. P. 10580-10585.
8. Gąska, D. & Margielewicz, J. Numeryczne modelowanie dynamiki podnoszonego ładunku. *Transport przemysłowy i maszyny robocze*. 2008. Vol. 1. P. 2-5. [In Polish: *Numerical modeling of dynamics of lifting the load*].
9. Ham, S.-H. & Roh, M.-I. & Lee, H. Simulation of load lifting with equalizers used in shipyards. *Automation in Construction*. 2016. Vol. 61. P. 98-111.
10. Haniszewski, T. Modeling the dynamics of cargo lifting process by overhead crane for dynamic overload factor estimation. *J. Vibroeng.* 2017. Vol. 19. No. 1. P. 75-86.
11. Haniszewski, T. Conception of the Arduino platform as a base for the construction of distributed diagnostic systems. *Scientific Journal of Silesian University of Technology. Series Transport*. 2016. Vol. 93. P. 31-40.
12. Kim, C.S. & Hong, K.S. & Kim, M.K. Nonlinear robust control of a hydraulic elevator: Experiment-based modeling and two-stage Lyapunov redesign. *Control Engineering Practice*. 2005. Vol. 13 (6). P. 789-803.
13. Kosucki, A & Malenta, P. The possibilities of reducing the operational load of hoisting mechanisms in case of dynamic hoisting. *Maintenance and Reliability*. June 2016. Vol. 18(3). P. 390-395.
14. Markusik, S. & Gąska, D. & Witaszek, K. Badania przyspieszeń i poziomów drgań w suwnicach pomostowych. *Scientific Journal of Silesian University of Technology. Series Transport*. 2007. Vol. 63. P. 181-186. [In Polish: *Study of acceleration and vibration levels in bridge cranes*].
15. Oguamanam, D.C.D. & Hansen, J.S. & Heppler, G.R. Dynamic response of an overhead crane system. *Journal of Sound and Vibration*. 1998. Vol. 213. No. 5. P. 889-906.
16. Ramli, L. & Mohamed, Z. & Abdullahi, A.M. & Jaafar, H.I. & Lazim, I.M. Control strategies for crane systems: A comprehensive review. *Mechanical Systems and Signal Processing*. 2017. Vol. 95. P. 1-23.
17. Reutov, A.A. & Kobishchanov, V.V. & Sakalo, V.I. Dynamic Modeling of Lift Hoisting Mechanism Block Pulley. *Procedia Engineering*. 2016. Vol. 150. P. 1303-1310.
18. Savković, M.M. & Bulatović, R.R. & Gašić, M.M. & Pavlović, G.V. & Stepanović, A.Z. Optimization of the box section of the main girder of the single-girder bridge crane by applying biologically inspired algorithms. *Engineering Structures*. 2017. Vol. 148. P. 452-465.
19. Wu, J.-J. Transverse and longitudinal vibrations of a frame structure due to a moving trolley and the hoisted object using moving finite element. *International Journal of Mechanical Sciences*. 2008. Vol. 50. No. 4. P. 613-625.

20. Zrnić, N.Đ. & Gašić, V.M. & Bošnjak, S.M. Dynamic responses of a gantry crane system due to a moving body considered as moving oscillator. *Archives of Civil and Mechanical Engineering*. 2015. Vol. 15. No. 1. P. 243-250.
21. PN-EN 13001-2: 2013. *Bezpieczeństwo dźwignic. Ogólne zasady projektowania. Część 2: Obciążenia*. Warszawa: Polski Komitet Normalizacyjny. 57 p. [In Polish: *Security of cranes. General principles for design. Part 2: Loads*. Warsaw: Polish Committee of Standardization].

Received 11.03.2017; accepted in revised form 23.11.2017